Hindawi
Mathematical Problems in Engineering
Volume 2022, Article ID 6908399, 13 pages
https://doi.org/10.1155/2022/6908399

Research Article

Research on Adaptive Sliding Mode Control of UVMS Based on Nonlinear Disturbance Observation

Wei Chen, Ming Wei, Yuhang Zhang, Di Lu, and Shilin Hu

School of Automation, Jiangsu University of Science and Technology, Zhenjiang 212003, China

Correspondence should be addressed to Wei Chen; cw1@just.edu.cn

Received 15 June 2022; Revised 10 August 2022; Accepted 20 August 2022; Published 13 September 2022

Academic Editor: Hamdi Gassara

The underwater vehicle manipulator system is a powerful tool for the exploration and development of marine resources. Due to the complexity of the marine environment, there are many disturbance factors and difficult to control. Taking the fixed depth control in hovering mode as an example, the vertical plane decoupling control model is established, and the adaptive sliding mode control method based on the disturbance observation is studied. The nonlinear disturbance observation is used to estimate the external unknown disturbance in real time, and the adaptive sliding mode method is used for compensation control. Simulation results show that the control method can effectively compensate for the sudden disturbance term, does not produce obvious trim motion, has strong robustness, and provides a reliable and stable base for the operation of the underwater manipulators. Finally, the operation experiments in the pool and real sea area under the disturbance condition are carried out, respectively. The experimental results show that the control effect is good and the stability is greatly improved compared with the traditional control method.

1. Introduction

The deep-sea environment presents the characteristics of high pressure, low temperature, and lack of oxygen. Humans cannot complete tasks in such harsh environments [1]. Therefore, it is necessary to use high-tech tools and methods to understand and explore the ocean [2, 3]. Underwater robots are undoubtedly a tool that can be relied upon on [4]. According to the degree of human intervention, underwater robots can be divided into cabled underwater vehicles (Remotely Operated Vehicle, ROV) and cableless underwater vehicles (Autonomous Underwater Vehicle, AUV) [5]. The basic functions of ROV/AUV are observation and inspection tasks, which are fully competent in support tasks such as entertainment and surveying, but underwater engineering operations require more implementation tools [6].

On the basis of ROV/AUV body equipped with manipulators, we can expand the operation field of underwater robots, which not only have the ability of underwater operation but also retains the characteristics of autonomy and flexibility of underwater robots [7, 8]. This control system is referred to as the underwater robot-manipulator system. According to the degree of intelligence, it is divided into manned type, remote control type, and autonomous type [5]. Manned UVMS is mainly used for deep-sea expedition missions in large research institutions or national research institutes. Compared with autonomous UVMS which is immature and has a higher risk of loss, remote-controlled UVMS develops an intelligent control system on the basis of ROV to achieve semiautonomous type underwater operations often appear to be both economical and realistic. The remote control UVMS only needs the operator to send the underwater operation task to the UVMS, and the actual operation can be coordinated by the underwater robot to complete the underwater operation task, and has the functions of autonomous navigation, autonomous obstacle avoidance, and autonomous operation [9, 10].

In recent years, a variety of control methods for UVMS have been proposed, including PID control, fuzzy control, adaptive control, robust control, sliding mode control, and neural network control. Comprehensive analysis shows that the PID control system is slow and its control accuracy is

limited [11]. Fuzzy control is a kind of empirical control, and its control accuracy depends on the perfection of summing up the experience. Although it has a strong anti-interference ability, it is rarely used in actual control systems alone, and most of them are used in combination with other control methods. Adaptive control is not very stable, and the power controller integration process is very time-consuming and usually cannot be completed online. The initial weight of the neural network-based method has high randomness and a long learning process, so it is difficult to apply in practice. In contrast, sliding mode control has the advantages of simple structure, fast response, small model parameter disturbance, and strong robustness [12]. For nonlinear systems like UVMS with external environmental interference, the sliding mode control method can provide a good solution. On this basis, domestic and foreign scholars have successively carried out arduous exploration and research and proposed a variety of sliding mode optimization control methods to improve the ability of UVMS underwater anti-disturbance operations [13].

In order to reduce the influence of UVMS in trajectory tracking control by external unknown disturbances and system coupling effects, PID sliding mode control [14], exponential method (SMC-EAL) sliding mode control [15], adaptive sliding mode control [16], inversion sliding mode control [17], integral sliding mode control [18], fuzzy sliding mode control [19], and other methods have been proposed one after another and achieved excellent control effects in the simulation stage. Wang et al. [20] combined sliding mode control and adaptive fuzzy control to form a multi-strategy fusion control, which solved the motion variable control problem of UVMS low-speed maneuvering, minimized the controller's dependence on the UVMS accurate model, and reduced the design cost of groundbreaking. In addition, in order to solve the disadvantage that the system state cannot converge to the equilibrium point in a limited time, the method based on or extended by terminal sliding mode control has gradually become the mainstream. Mobayen et al. [21] proposed a continuous nonsingular fast terminal sliding mode control with time delay estimation, which can ensure satisfactory tracking control performance and good robustness under lumped uncertainty conditions. The effectiveness of this method is verified in the pool experiment of the seven-degree-of-freedom UVMS. Mofid et al. [22] proposed a fuzzy terminal sliding mode control method with time delay estimation, which focuses on using fuzzy rules to adaptively adjust the terminal sliding mode surface to get rid of the internal and external uncertainties caused by complex dynamics. To sum up, although sliding mode control has made significant breakthroughs in the application of nonlinear system control, the main problem of UVMS is to estimate the lumped uncertainty disturbance on the basis of getting rid of the constraints of dynamics. Many scholars have begun to introduce disturbance observers to improve the sliding-mode control performance, and this method provides a novel solution for studying UVMS high-precision control under perturbed conditions.

Nonlinear Disturbance Observation (NDO) is an effective control method to deal with system model mismatch and external disturbance [23, 24]. The NDO has the advantages of simple algorithm and easy engineering implementation [25]. It can estimate factors such as external disturbance and parameter uncertainty in real time and use this estimated value to compensate the influence of aggregate disturbance on the control accuracy of the servo control system. Attenuate the high-frequency chattering caused by aggregation perturbation to sliding mode control, and a new adaptive algorithm is used to estimate the sliding mode switching gain online in real time to avoid the sliding mode chattering problem caused by excessive gain. It has gradually become a popular method for anti-disturbance control of nonlinear redundant systems and is widely used in nonlinear disturbance environments [26]. Systems such as permanent magnet synchronous motors, unmanned aerial vehicles, launch vehicles, helicopters, and surface unmanned ships [27].

In the research of UVMS control methods, disturbance observation control has also made some progress, such as fast terminal sliding mode control based on a nonlinear disturbance observer, nonsingular a fixed-time terminal sliding mode control with a fixed-time disturbance observer, and nonsingular fixed-time terminal sliding mode control with disturbance estimator [28, 29]. Methods such as singular fast fuzzy terminal sliding mode control and fuzzy sliding mode active disturbance suppression control based on extended state observer have been proposed and verified accordingly. Relying on its powerful nonlinear approximation ability, the disturbance observer can not only estimate the external disturbance but also estimate the dynamic changes of the system and the uncertainty of the model [30]. Combined with the strong robustness of sliding mode control, it can be used in transient response and stability [31]. State accuracy, convergence speed, and robustness ensure that the given trajectory is reached and meet the requirements of underwater refined operations.

2. Dynamic Modeling of UVMS

Through the corresponding analysis of UVMS and operating environment, the dynamic model of the underwater robot under disturbance conditions is established. Among them, the lumped uncertain disturbances in the actual underwater environment are considered when modeling, including fluid dynamics (additional mass, damping force, and restoring force), underwater environmental disturbance forces, and coupling moments between systems, which are conducive to a reasonable judgment of UVMS effectiveness of control methods.

2.1. UVMS Kinetic Model. According to Newton's law of dynamics and the law of moment of momentum, the nonlinear dynamic equation of the six-degree-of-freedom motion of the underwater vehicle body is usually expressed in the body coordinate system as follows:

$$M_{RB}\dot{\nu} + C_{RB}(\nu)\nu = \tau. \tag{1}$$

Among them, M_{RB} is the mass inertia matrix of the body coordinate system, which is determined by the body mass distribution, and C_{RB} is the Coriolis force and centripetal force matrix.

The general formula of the external force and external torque on the underwater robot body (τ) can be written in the form of the sum of various forces and torques:

$$\tau = \tau_H + \tau_R + \tau_P + f. \tag{2}$$

Among them, τ_H is the hydrodynamic force, including the inertial force generated by the additional mass of the fluid, the Coriolis force, the centripetal force, and the fluid damping force, τ_R is the gravity and buoyancy, τ_P is the thrust and thrust moment provided by the propeller, and f is the unknown external environment forces.

2.2. Thrust and Thrust Moment of the Propeller. In order to better analyze, the six-degree-of-freedom motion control of UVMS when modeling, it is necessary to calculate the corresponding vector thruster system in advance for the UVMS power distribution method. The installation positions and angles of the four thrusters installed in vector symmetry in the space coordinate system are shown in Figure 1:

The positive direction of its thrust is at an angle of 15° with O_bX_b , and the total thrust produced by the propeller is expressed as follows:

$$\begin{cases} TX_h = -T_1 \cos\alpha - T_2 \cos\alpha, \\ TY_h = T_1 \sin\alpha - T_2 \sin\alpha, \\ TZ_h = 0. \end{cases} \tag{3}$$

In the formula, T_1、 T_2 represent the thrust of the horizontal thruster, α represents the vector angle formed by the horizontal thruster and the ob axis, and TX_h、 TY_h、 TZ_h represent the combined thrust of the horizontal thruster.

Referring to Figure 2 and Table 1, the UVMS thrust matrix after removing the pitch degrees of freedom can be expressed as follows:

$$\tau = \begin{bmatrix} X \\ Y \\ Z \\ K \\ N \end{bmatrix} = \begin{bmatrix} \cos\alpha & \cos\alpha & 0 & 0 \\ \sin\alpha & -\sin\alpha & \sin\beta & -\sin\beta \\ 0 & 0 & -\cos\beta & -\cos\beta \\ 0 & 0 & L_6\cos\beta & L_6\cos\beta \\ -L_1\cos\alpha & -L_1\cos\alpha & 0 & 0 \end{bmatrix} \begin{bmatrix} f_1 \\ f_2 \\ f_3 \\ f_4 \end{bmatrix} = B(a)T. \tag{4}$$

The thrust required for each thruster to achieve its own degree of motion can be calculated by the following formula:

$$\begin{aligned} f &= B_1^+ \tau_{p1}, \\ B_1^+ &= B_1^T \left(B_1 B_1^T\right)^{-1}. \end{aligned} \tag{5}$$

2.2.1. Water Power. The underwater robot body will face additional mass, damping (resistance, lift, lateral force), restoring force (weight, buoyancy), etc. due to hydrodynamic effects during movement:

$$\tau_H = -M_{AM}\dot{v} - C_{AM}(v)v - D(v)v - g(\eta). \tag{6}$$

Additional mass: When the underwater robot body is running in a fluid environment, it will inevitably drive part of the water flow attached to the periphery of the robot, causing this part of the water flow to move with the underwater robot body, thus generating additional mass.

Any object motion will produce inertia. In the rotating system, the Coriolis and centripetal terms of UVMS are expressed as $\mathbf{C}_{AM}$.

Viscous damping: It mainly comes from the linear friction of the laminar boundary layer, the secondary friction of the turbulent boundary layer, and the secondary resistance caused by eddy currents. Viscous resistance and torque are the equations of the relative fluid-motion relationship. According to the second-order Taylor series expansion, the viscous resistance of the underwater robot body can be expressed as follows:

$$f_v = -D_L x_\tau - D_q(x_\tau). \tag{7}$$

D_L: linear damping coefficient matrix

$$D_L = \operatorname{diag}\left(X_u, Y_v, Z_w, K_p, M_q, N_r\right). \tag{8}$$

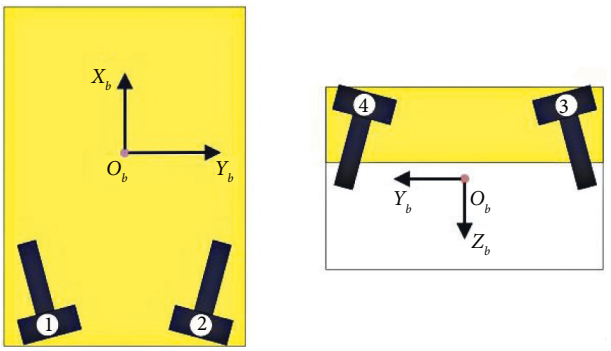

Figure 1: UVMS thruster power layout.

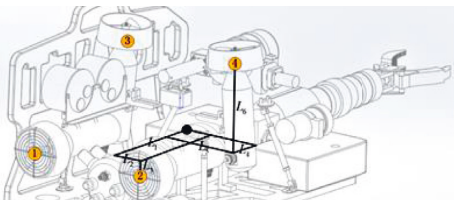

Figure 2: Three-dimensional distribution of propeller.

Table 1: Configuration parameters of UVMS thruster.

Number	Describe	X (m)	Y (m)	Z (m)	Vector angle
1	Stern left horizontal	$-L_1$	L_2	L_3	15° to O_bX_b
2	Stern right horizontal	$-L_1$	$-L_2$	L_3	15° to O_bX_b
3	Stern left vertical	$-L_4$	L_5	$-L_6$	15° to O_bZ_b
4	Stern right vertical	$-L_4$	$-L_5$	$-L_6$	15° to O_bZ_b

D_L: nonlinear damping coefficient matrix

$$D_q(x_\tau) = \mathrm{diag}\left(X_{u|u|}|u|, Y_{v|v|}|v|, Z_{w|w|}|w|, K_{p|p|}|p|, M_{q|q|}|q|, N_{r|r|}|r|\right). \tag{9}$$

Froude–Krylov wave force: the force exerted by the unstable pressure field formed by the undisturbed wave, the Froude–Krylov force and moment can be expressed as follows:

$$f_{FK} = M_{FK}\dot{u}_f. \tag{10}$$

2.2.2. Gravity and Buoyancy. The combined effect of gravity and buoyancy is called restoring force/moment. After the underwater robot body is fully submerged, due to the action of the floating body, W (gravity term), and B (buoyancy term) will generate a restoring force/moment parallel to the z-axis of the Earth coordinate system. In the body coordinate system, the restoring force/moment can be decomposed into components on each axis.

Through the neutral buoyancy test, to ensure that the gravity and buoyancy are the same, the expressions of restoring force and moment can be expressed as follows:

$$g(x) = \begin{bmatrix} 0 \\ 0 \\ 0 \\ (y_I W - y_B B)\cos\theta\cos\phi + (z_I W - z_B B)\cos\theta\sin\phi \\ -(x_I W - x_B B)\cos\theta\cos\phi - (z_I W - z_B B)\sin\theta \\ (x_I W - x_B B)\cos\theta\sin\phi + (y_I W - y_B B)\sin\phi \end{bmatrix}. \tag{11}$$

2.2.3. Unknown External Environmental Forces

(1) System Uncertainty Disturbance. System uncertainty disturbances are mainly caused by parameterized uncertainties and unmodeled dynamics of the system. The parametric uncertainty is due to the change of hydrodynamic coefficients during the movement. The unmodeled dynamics of the system is because the hydrodynamics are expanded according to the second-order Taylor series during the modeling process, and the neglected high-order terms will cause certain errors.

(2) External Wave Current Disturbance. The near water surface is mainly disturbed by waves, and the distance from the water surface is mainly disturbed by currents. For the near-water surface environment, the disturbance of the second-order wave force is the main influencing factor, and the model can be expressed as follows:

$$\tau_{\mathrm{wave}i} = \frac{K_{wi}s}{s^2 + 2\lambda_i w_{ei}s + w_{ei}^2}w_i + d_{wi}, \dot{d}_{wi} = w_{di}, \tag{12}$$

w_i, w_{di}: Gaussian white noise, K_{wi}: Spectral amplitude, λ_i, w_{ei}: Spectral parameter pair, d_{wi}: Low frequency spectrum drag.

For the water flow in the underwater environment, it can be regarded as the fluid circulation system in the horizontal and vertical directions. It is caused by the friction force of the tide and wind and the change of fluid density. It is a process of low-frequency slow change, and its flow velocity and the interference force produced. Can be described as follows:

$$v_c = -\mu v_c + \omega\tau_{\mathrm{current}} = C_A v_c + D v_c, \tag{13}$$

v_c: Ocean current velocity vector, μ: Positive definite diagonal matrix, ω: Gaussian white noise vector, C_A, D: Constant parameter.

(3) Unstructured Random Disturbance. Unstructured random interference refers to the noise interference in the sensor measurement, and the actual underwater environment is complex and changeable, and the calibration accuracy of the measurement equipment is limited, resulting in the measurement system inevitably being polluted by various noises, introducing nonstationary random errors into the measurement so that the frequency of the measurement signal changes with time. Combining the effects of the abovementioned time-varying disturbances of external wave currents and measurement noise disturbances, the complex environmental disturbances can be described as follows:

$$d = J(\eta)\left(\tau_{\mathrm{wave}i} + \tau_{\mathrm{current}}\right), \dot{\tau}_{\mathrm{current}} = -T\tau_{\mathrm{current}} + \Lambda w, \tag{14}$$

η: Pose vector, $w(w \in R^6)$: Zero mean Gaussian white noise vector, $T(T = \mu \in R^{6\times6})$: Positive definite diagonal matrix, $\Lambda(\Lambda = C_A + D \in R^{6\times6})$: Gaussian white noise gain matrix.

In order to better summarize the dynamic model of the underwater robot, we regularize the hydrodynamic force, restoring force data, and external unknown environmental forces into external lumped interference items:

$$k = \mathrm{diag}[f_X, f_Y, f_Z, f_K, f_M, f_N]^T. \tag{15}$$

Considering the uncertainty of model parameters, the dynamic equation of the underwater vehicle can be summarized as follows:

$$M\dot{v} + C(v)v + D(v)v + g(\eta) + k = \tau_p. \tag{16}$$

The parameters in this model are as follows:

$$\begin{aligned} M &= M_{RB} + M_{AM} + \Delta M, \\ C(v) &= C_{RB}(v) + C_{AM}(v) + \Delta C(v), \\ D(v) &= 2D_L + D_q(x_\tau) + \Delta D(v). \end{aligned} \tag{17}$$

3. UVMS Modeling Analysis

The ocean is low-temperature and high-pressure, complex and changeable, and more robust control methods are needed to achieve UVMS operation control under disturbance conditions. When studying control methods, not only the accuracy of the job task must be considered but also the influence of the external environment. Therefore, it is particularly important to choose a method that meets the control objectives and operating environment. Compared

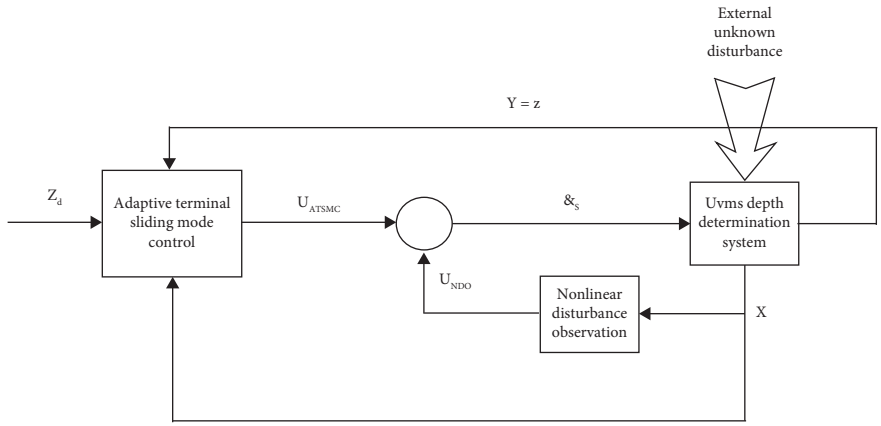

Figure 3: UVMS antidisturbance motion control system.

with the manipulator system, unknown disturbances from the outside have a great influence on the body of the underwater robot, so the hovering accuracy of UVMS directly affects the gripping performance of the manipulator. The hover mode of UVMS includes fixed depth control and fixed bow control. Taking the fixed depth system as an example, based on the establishment of the UVMS model under disturbance conditions, the research on the anti-disturbance control method of UVMS motion is carried out to provide a stable base platform for the subsequent manipulator.

3.1. UVMS Fixed Depth Adaptive Sliding Mode Control Based on Nonlinear Disturbance Observation. Adaptive sliding mode control can no longer meet the control goal under a relatively small control amount. The introduction of a nonlinear disturbance observation method can estimate the internal and external unknown disturbance values in real time, calculate the input compensation amount, and make up for the shortcomings of adaptive sliding mode control in dealing with sudden unknown disturbances.

The basic idea of the built depth antidisturbance control system is shown in Figure 3:

Using the control concept of the combination of nonlinear disturbance observation, adaptive control, and sliding mode control, the UVMS depth control system is used as the research object, and the antidisturbance control method is researched. Sliding mode control is chosen as the basic control method, which is widely used in time-varying nonlinear systems with unmodeled dynamics, uncertain model parameters, and susceptible to external disturbances. The nonlinear disturbance observation method can perform online estimation of system uncertainty and external environmental interference based on the information provided by the existing system. The adaptive algorithm can effectively reduce the disturbance estimation error and improve the disturbance observation accuracy. Sliding mode control has the advantages of simple structure and insensitive to parameter changes, but it is also prone to chattering problems. Therefore, the saturation function is introduced to weaken the chattering of sliding mode control.

3.1.1. Depth Control Model Design. The dynamic model of the underwater robot under the condition of external lumped disturbance is analyzed for motion decoupling. The addition of the external lumped disturbance item makes the decoupled depth control system more comprehensive.

The kinetic model of UVMS under disturbance conditions is as follows:

$$\begin{cases} \dot{\eta} = J(\eta_2)v, \\ M\dot{v} + C(v)v + D(v)v + g(\eta_2) + k = \tau_p. \end{cases} \tag{18}$$

UVMS is equipped with a front manipulator. Although the center of buoyancy is changed by adding a floating body to the bow, it destroys the stability of the original floating body to a certain extent. This will produce a roll angle and a pitch angle, so when we consider the depth fix mode, we must comprehensively consider the vertical motion and pitch motion after UVMS decoupling, that is, the four vectors of UVMS (z, θ, w, q). The UVMS kinematic models established under different reference coordinate systems are shown in Figure 4.

The vertical motion after decoupling is expressed as follows:

$$\begin{cases} \dot{z} = w\cos\theta - u\sin\theta, \\ m\left(\dot{w} - uq - x_G\dot{q} - z_G q^2\right) = Z_{\dot{q}}\dot{q} + Z_{\dot{w}}\dot{w} + Z_{uq}uq \\ \quad + Z_{uu}uw + Z_{w|w|}w|w| + Z_{q|q|}q|q| \\ \quad + (W - B_o)\cos\theta + Z_{ut}u^2\delta_s. \end{cases} \tag{19}$$

The trim motion after decoupling is expressed as follows:

$$\begin{cases} \dot{\theta} = q \\ I_{yy}\dot{q} + m\left[x_G(uq - \dot{w}) + z_G wq\right] = M_{\dot{q}}\dot{q} + M_{\dot{w}w}\dot{w} \\ \quad + M_{uq}uq + M_{uw}uw + M_{w|w|}w|w| + M_{q|q|}q|q| \\ \quad + -(x_G W - x_B B_o)\cos\theta - (z_G W - z_B B_o)\sin\theta \\ \quad + M_{uu}u^2\delta_s + k. \end{cases} \tag{20}$$

In view of the actual situation, we simplified the above model, assuming the submerged speed $\omega \approx 0, \dot{\omega} \approx 0$; the

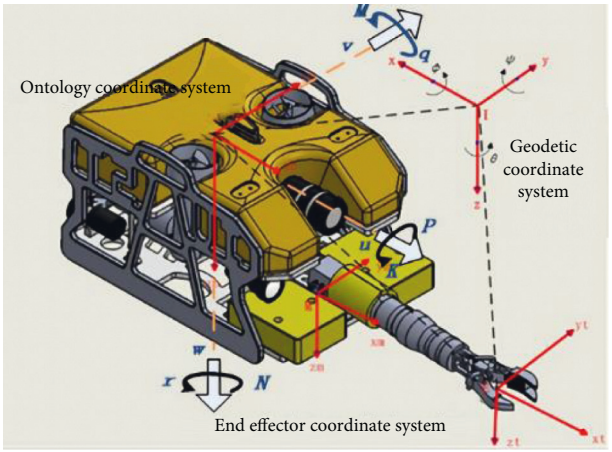

FIGURE 4: UVMS coordinate system and degree of freedom parameters.

center of mass of the geodetic coordinate system (x_G, y_G, z_G); buoyancy center of the geodetic coordinate system (x_B, y_B, z_B).

According to the relevant spatial definition, $x_G = x_B = z_B = 0$.

The vertical motion model can be simplified as follows:

$$\begin{cases} \left(I_{yy} - M_{\dot{q}}\right)\dot{q} = M_{uq}uq + M_{q|q|}q|q| - x_G W\cos\theta \\ \quad -z_G W\sin\theta + M_{uu}u^2\delta_S + k, \\ \dot{\theta} = q, \\ \dot{z} = -u\sin\theta. \end{cases} \tag{21}$$

Definition $x_1 = z, x_2 = \theta, x_3 = q$, The simplified kinetic model is as follows:

$$\begin{cases} \dot{x}_1 = -u\sin x_2, \\ \dot{x}_2 = x_3, \\ \dot{x}_3 = M_1 x_3 + M_2 x_3|x_3| + M_3\cos x_2 \\ \quad +M_4\sin x_2 + M_5\delta_S + K. \end{cases} \tag{22}$$

In this formula:

$$\begin{aligned} M_1 &= \frac{M_{uq}u}{\left(I_{yy} - M_{\dot{q}}\right)}, \\ M_2 &= \frac{M_{q|q|}}{\left(I_{yy} - M_{\dot{q}}\right)}, \\ M_3 &= -\frac{x_G W}{\left(I_{yy} - M_{\dot{q}}\right)}, \\ M_4 &= -\frac{z_G W}{\left(I_{yy} - M_{\dot{q}}\right)}, \\ M_5 &= \frac{M_{uu}u^2}{\left(I_{yy} - M_{\dot{q}}\right)}, \\ K &= \frac{k}{\left(I_{yy} - M_{\dot{q}}\right)}, \end{aligned} \tag{23}$$

K is the unknown disturbance outside the system.

3.2. Research on Adaptive Sliding Mode Control Method

3.2.1. Nonlinear Disturbance Observation Control. The nonlinear disturbance observation method will estimate in real time the unknown external disturbances received by the UVMS during depth control. Estimated value of external unknown disturbance $\hat{k} = (I_{yy} - M_{\dot{q}})\hat{K}$.In order to estimate $\hat{K}$ and obtain the external unknown disturbance value by conversion, define the UVMS state variable $x = [x_1, x_2, x_3]^T$ to obtain the vector form of the UVMS vertical plane system model:

$$\dot{x} = A(x) + B(x)\delta_S + C(x)K. \tag{24}$$

In this formula:

$$\begin{aligned} A(x) &= \left[-u\sin x_2 \;\; x_3 \;\; M_1 x_3 + M_2 x_3|x_3| + M_3\cos x_2 + M_4\sin x_2\right]^T, \\ B(x) &= \left[0 \;\; 0 \;\; M_5\right]^T, \\ C(x) &= \left[0 \;\; 0 \;\; 1\right]^T. \end{aligned} \tag{25}$$

Consider the basic composition of the nonlinear disturbance observation method:

$$\begin{cases} \hat{d}_{M-A} = m + p(x), \\ \dot{m} = L\left(-F(x) - Q_1(x)\delta_s - Q_2(x)\left(m + p(x)\right)\right). \end{cases} \tag{26}$$

In this formula:

$$p(x) = p_1 x_1 + p_2 x_2 + p_3 x_3 \left(p_1 > 0, p_2 > 0, p_3 > 0\right). \tag{27}$$

The following nonlinear interference observer is established with reference to the basic structure:

$$\begin{cases} m = \hat{K} - f(x), \\ \dot{m} = -L\left(A(x) + B(x)\delta_s + C(x)\left(m + f(x)\right)\right). \end{cases} \tag{28}$$

In this formula:

$$\begin{aligned} f(x) = f_1 x_1 + f_2 x_2 + f_3 x_3, \left(f_1 > 0, f_2 > 0, f_3 > 0, L \right. \\ \left. = \frac{\partial f(x)}{\partial x} = \left[f_1 \;\; f_2 \;\; f_3\right]\right). \end{aligned} \tag{29}$$

In the absence of prior knowledge, since the range of unknown disturbances cannot be effectively estimated, it is assumed that the dynamic changes of disturbances are slower than the dynamic changes of UVMS. which is $\dot{K} = 0$. The observation error of interference is $\tilde{K} = K - \hat{K}$.

$$\left\{\dot{\tilde{K}} = \dot{K} - \dot{\hat{K}} = -\dot{\hat{K}}, \dot{\hat{K}} = \dot{m} + \dot{f}(x) = -LC(x)\tilde{K}.\right. \tag{30}$$

Due to that $-LC(x)\tilde{K} = -f_3\tilde{K}$ and $f_3 > 0$. Therefore, the error value of the nonlinear disturbance observer converges to zero, that is, the observed value gradually tends to the actual external unknown disturbance value.

The control quantity output by the nonlinear disturbance observer is expressed as follows:

$$u_{NDO} = \frac{1}{M_5}\widehat{K}. \tag{31}$$

3.2.2. Adaptive Sliding Mode Control with Nonlinear Observation Method. On the basis of constructing a nonlinear disturbance observation method, UVMS can be transformed as follows:

$$\begin{cases} \dot{x}_1 = -u\sin x_2, \\ \dot{x}_2 = x_3, \\ \dot{x}_3 = M_1 x_3 + M_2 x_3|x_3| + M_3\cos x_2 \\ \quad +M_4\sin x_2 + M_5\delta_S + \widehat{K} + \widetilde{K}. \end{cases} \tag{32}$$

The estimated error value of the external unknown disturbance $\widehat{K}$ is obtained by the nonlinear disturbance observation method. In order to improve the control performance, the corresponding control rate design must be carried out. For the convenience of description, let $\widetilde{K} = J$. Further estimate the estimated error value of the external unknown disturbance: $\widetilde{J} = J - \widehat{J}$. The same as the design of the disturbance observation method, the error estimate is slower than the rate of change of the UVMS control system, namely $\dot{J} = 0$. The dynamic surface definition and Lyapunov function of vertical motion are expressed as follows:

$$\begin{aligned} S_1 &= z - z_d = x_1 - z_d, \\ V_1 &= \frac{1}{2}S_1^2. \end{aligned} \tag{33}$$

Define the virtual control input α_1 as follows:

$$\alpha_1 = k_1 S_1 - \frac{1}{u}\dot{z}_d, k_1 > 0. \tag{34}$$

The definition of the dynamic surface of the trim motion and the Lyapunov function are expressed as follows:

$$\begin{aligned} S_2 &= x_2 - \alpha_1, \\ V_2 &= V_1 + \frac{1}{2}S_2^2. \end{aligned} \tag{35}$$

Define the virtual control input α_2 as follows:

$$\alpha_2 = -k_2 S_2 + \dot{\alpha}_1 + uS_1. \tag{36}$$

The dynamic surface of the angular velocity tracking error of the trim motion is defined as follows:

$$S_3 = x_3 - \alpha_2. \tag{37}$$

Finally, the terminal sliding surface is integrated as follows:

$$\sigma = S_3 + \int_0^t \left[m_1 |S_3|^a \operatorname{sign}(S_3) + m_2 |S_3|^\beta \operatorname{sign}(S_3) \right] dt. \tag{38}$$

Among them, m_1, m_2, α, β is the positive definite coefficient, and the sign function is as follows:

$$\operatorname{sign}(S_3) \begin{cases} = 1, & S_3 > 0, \\ = 0, & S_3 = 0, \\ = -1, & S_3 < 0. \end{cases} \tag{39}$$

Due to the problems of time lag, space lag, system inertia, system delay, and measurement error in the actual system, a saw tooth trajectory is formed on the sliding mode surface, so the sliding mode control chattering phenomenon always exists. Chattering not only affects control accuracy, increases energy consumption but also easily stimulates high-frequency unmodeled dynamics in the system, destroys system energy, and even damage system components.

Excessive switching gain δ will cause chattering phenomenon when the system approaches the sliding mode surface, and the introduction of saturation function $\operatorname{sat}(s, \Delta)$ can effectively alleviate this phenomenon:

$$\operatorname{sat}(s, \Delta) = \begin{cases} \dfrac{s}{\Delta}, & |s| \le \Delta, \\ \operatorname{sign}(s), & |s| \ge \Delta. \end{cases} \tag{40}$$

The value of Δ is determined by the switching gain δ. The sliding mode controller established above can be updated to

$$\sigma = S_3 + \int_0^t \left[m_1 |S_3|^a \operatorname{sat}(S_3, \Delta) + m_2 |S_3|^\beta \operatorname{sat}(S_3, \Delta) \right] dt. \tag{41}$$

In order to obtain the estimated value $\widehat{J}$, the adaptation rate can be designed as follows:

$$\dot{\widehat{J}} = \lambda\sigma, \lambda > 0. \tag{42}$$

The control quantity output by the adaptive terminal sliding mode controller is

$$u_{ATSMC} = -\frac{1}{M_5}\left(M_1 x_3 + M_2 x_3|x_3| + M_3\cos x_2 + M_4\sin x_2 + \widehat{J} + m_1|S_3|^a \operatorname{sat}(S_3, \Delta) + m_2|S_3|^\beta \operatorname{sat}(S_3, \Delta) + (\widehat{J} + \gamma)\operatorname{sgn}(\sigma) \right). \tag{43}$$

Finally, the output of the adaptive sliding mode controller based on the nonlinear disturbance observation method is expressed as follows:

$$\delta_S = -\frac{1}{M_5}\left(M_1 x_3 + M_2 x_3|x_3| + M_3\cos x_2 + M_4 \sin x_2 + \hat{J} + \hat{K} - \dot{\alpha}_2 + m_1|S_3|^a \mathrm{sat}(S_3,\Delta) + m_2|S_3|^\beta \mathrm{sat}(S_3,\Delta) + (\delta+\gamma)\mathrm{sgn}(\sigma)\right). \tag{44}$$

The Lyapunov function of the entire controller is

$$V_3 = \frac{1}{2}\sigma^2 + \frac{1}{2}\tilde{K}^2 + \frac{1}{2\lambda}\tilde{J}^2. \tag{45}$$

3.3. Stability Analysis. In order to study the convergence of depth trajectory tracking, each sliding surface of the control method should be analyzed. In the actual operation engineering, the UVMS trim angle $x_2 = \theta$ changes in a relatively small range, that is $\cos x_2 \longrightarrow 1$. For the convenience of verification, it is assumed that $\cos x_2 = 1$, $\sin x_2 = x_2$.

$$\dot{V}_1 = S_1\dot{S}_1 = S_1(\dot{x}_1 - \dot{z}_d) = S_1(-ux_2 - \dot{z}_d) = -S_1 u(S_2 + \alpha_1) - S_1\dot{z}_d = -S_1 u\left(S_2 + k_1 S_1 - \frac{1}{u}\dot{z}_d\right) - S_1\dot{z}_d = -uS_1S_2 - k_1 uS_1^2. \tag{46}$$

In the above formula, u is the forward and backward speed of UVMS, and the default is $u > 0$. In summary, to ensure the stability of the above vertical movement, $S_2 = 0$ must be guaranteed.

Analyze the dynamic surface of trim motion:

$$\dot{V}_2 = \dot{V}_1 + S_2\dot{S}_2 = -uS_1S_2 - k_1uS_1^2 + S_2(x_3 - \dot{\alpha}_1) = -uS_1S_2 - k_1uS_1^2 + S_2(S_3 - k_2S_2 + \dot{\alpha}_1 + uS_1 - \dot{\alpha}_1) = -k_1uS_1^2 + S_2S_3 - k_2S_2^2. \tag{47}$$

When $S_3 = 0$, it can be seen that $\dot{V}_2 \le 0$, that is, the sliding surface of the trim motion gradually converges to zero. When the current assumption is established, the angular velocity tracking error of the pitch motion will gradually converge to zero, and the stability of the sliding mode surface S_3 will be judged:

$$\begin{aligned}\dot{V}_3 &= \sigma\dot{\sigma} + \tilde{K}\dot{\tilde{K}} + \frac{1}{\lambda}\tilde{J}\dot{\tilde{J}} = \sigma\left(\dot{S}_3 + m_1|S_3|^a \mathrm{sat}(S_3,\Delta) + m_2|S_3|^\beta \mathrm{sat}(S_3,\Delta)\right) + \tilde{K}(-f_3\tilde{K}) + \frac{1}{\lambda}\tilde{J}(-\dot{\hat{J}}) \\ &= \sigma\left(\left(M_1x_3 + M_2x_3|x_3| + M_3 + M_4x_2 + M_5\delta_S + \hat{K} + \tilde{K} - \dot{\alpha}_2\right) + m_1|S_3|^a \mathrm{sat}(S_3,\Delta) + m_2|S_3|^\beta \mathrm{sat}(S_3,\Delta)\right) \\ &\quad + \tilde{K}(-f_3\tilde{K}) - \frac{1}{\lambda}\tilde{J}\dot{\hat{J}} = \sigma(-\hat{J} - (\delta+\gamma)\mathrm{sgn}(\sigma) + \tilde{K}) - f_3\tilde{K}^2 - \frac{1}{\lambda}\tilde{J}(\lambda\sigma) = -\sigma(\delta+\gamma)\mathrm{sgn}(\sigma) - f_3\tilde{K}^2.\end{aligned} \tag{48}$$

In summary, when $\sigma = 0$, it can be seen that $\dot{V}_3 \le 0$, the terminal sliding mode surface S_3 gradually converges to zero. That is, the sliding mode surface S_2 and S_1 also converge to zero accordingly. Therefore, it can be proved that the designed control method tends to be stable in the end.

4. Analogue Simulation

In order to verify the performance of the adaptive sliding mode control method based on nonlinear disturbance observation in the depth control of UVMS, simulation experiments are carried out. The parameters of the nonlinear disturbance observer are as follows: $f_1 = f_2 = f_3 = 1$

The parameters of the adaptive terminal sliding mode controller are as follows: $k_1 = 1.5, k_2 = 2, k_1 = 1.5, m_1 = m_2 = 2.1, \alpha = 0.6, \beta = 1.2, \lambda = 0.1$. For the UVMS fixed-depth control model, the fluid dynamic parameters refer to Peng Shengquan's "Underwater Robot-Manipulator System Motion Planning and Control Technology Research," and the physical parameters are shown as Table 2:

Since the vertical dynamic model only considers $x = [z, \theta, w, q]^T$. The initial state of UVMS is expressed as follows: $x = [0, 0, 0, 0]^T$.The duration of external unknown disturbance is 20 s–40 s. The amount of disturbance is expressed as follows: $k = 5\sin(0.1t) + 6\cos(0.3t)$.

Table 2: Physical parameters.

Number	Value
x_B, y_B, z_B	0 m
x_G, y_G	0 m
z_G	−0.05 m
m	18.7 kg
I_{yy}	2 kgm^2
W	184 N
B_o	190 N

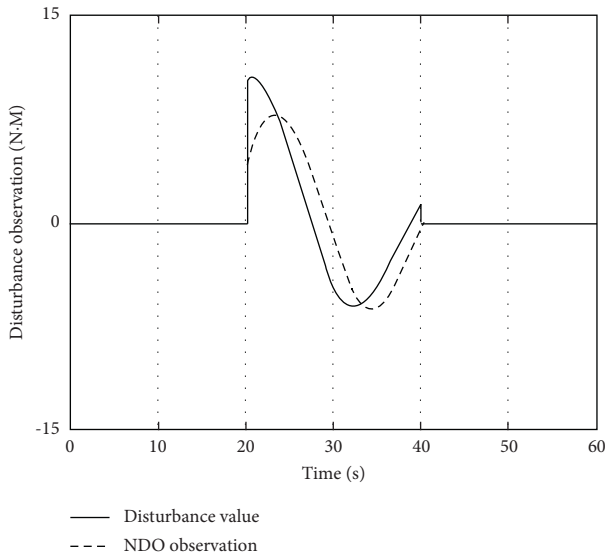

Figure 5: Disturbance tracking observation.

The biggest disturbance that UVMS faces when operating in real waters is the unknown amount of interference from the outside world, so the abovementioned disturbance functions are individually tracked and tested. As shown in Figure 5, in the face of the sudden disturbance at the 20th second, the nonlinear disturbance observer responded in time, but the value of the first disturbance was not captured when the upper limit of the first disturbance appeared, and the subsequent disturbances were tracked within 2 seconds and the disturbance value was tracked. Limit and better complete the tracking of the disturbance and provide a better control performance basis for subsequent compensation.

In order to meet the requirements of actual underwater grasping operations, the simulation is static depth setting, and the depth setting is set to 30 m. The adaptive sliding mode method with the intervention of a nondisturbing observer is compared with the traditional adaptive sliding mode method, and the simulation is compared. The graph analysis is as follows:

Analyzing Figure 6, the intervention of the nonlinear disturbance observer improves the response speed of depth tracking and realizes stable control within 10 s. Overshoot occurs in adaptive sliding mode control, and the intervention of nonlinear disturbance observer makes the depth tracking curve smooth. There is no obvious change in the disturbance interval, showing good depth tracking

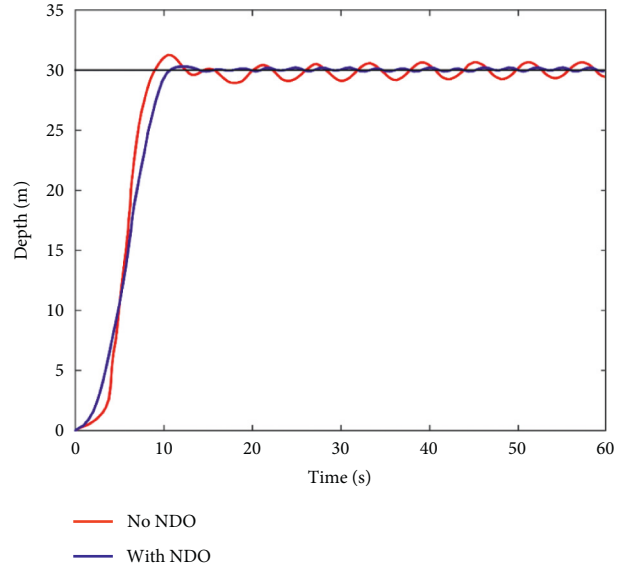

Figure 6: UVMS depth output comparison chart.

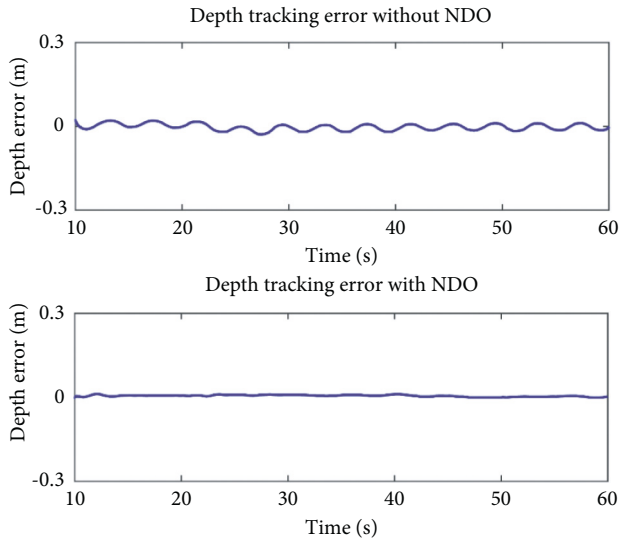

Figure 7: UVMS depth error comparison chart.

performance. It can also be clearly seen from the depth tracking error graph in the figure below that the adaptive sliding mode compensation performance after the nonlinear disturbance observer captures the disturbance is excellent, the curve is smooth as a whole, and the expected compensation control effect is achieved.

As shown in Figures 7 and 8, UVMS acquires state variables in real time during the process of tracking the target depth. In the disturbance simulation interval, both the trim angle and the trim angular velocity are affected to varying degrees, but the overall variables remain in the ±5° interval. Therefore, it can be seen that the open-frame structure of the floating body is beneficial to the maintenance of positive stability, and the degree of freedom of the UVMS pitch is passively adjusted. Although the installation of additional power components can achieve active compensation, it is often accompanied by an increase in

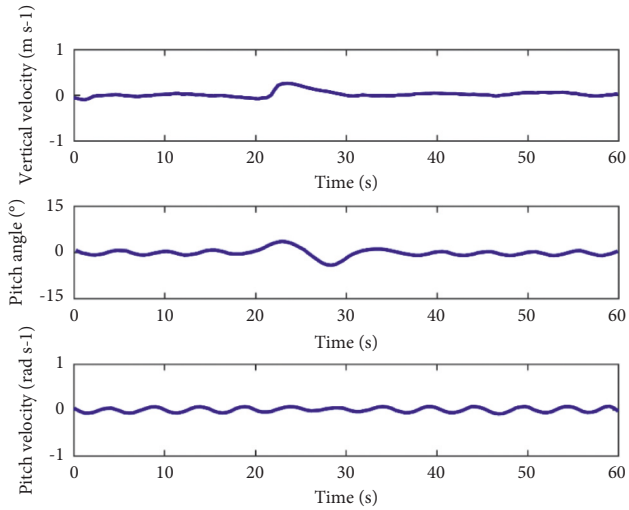

Figure 8: Change trend of UVMS depth determination control state.

Figure 9: UVMS pool test.

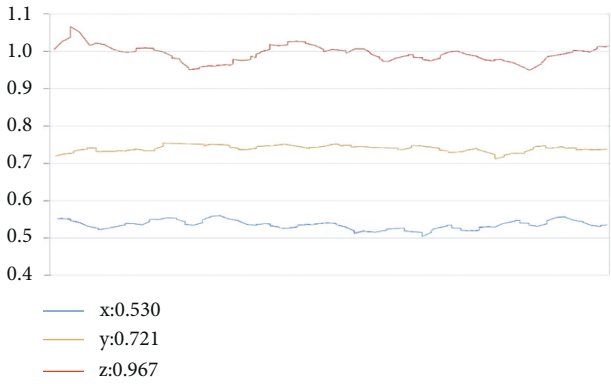

Figure 10: Adaptive sliding mode depth control data chart.

redundancy and complexity. In the stability analysis of the abovementioned fixed-depth controller, the hypothesis: $\cos x_2 = 1$, $\sin x_2 = x_2$ is also disproved. In addition, the vertical speed almost tends to zero during the entire control process, and the speed when the disturbance emerges is also quickly corrected by the control method, which satisfies $w = 0, \dot{w} = 0$. In summary, it can be seen that the adaptive

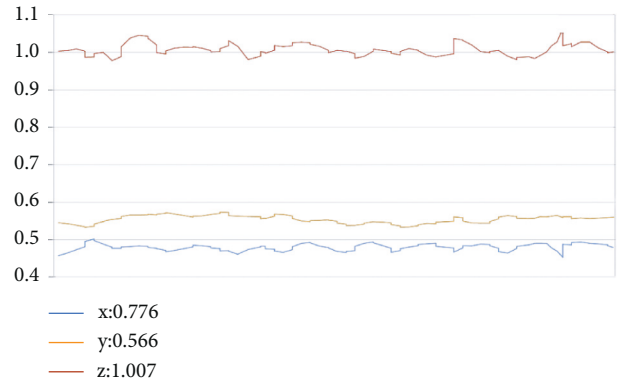

Figure 11: Data chart of adaptive sliding mode depth determination control with nonlinear disturbance observation.

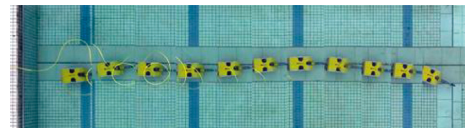

Figure 12: Adaptive sliding mode fixed bow control data graph.

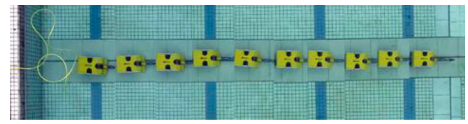

Figure 13: Data diagram of adaptive sliding mode bow control based on nonlinear disturbance observation.

sliding mode method that introduces the nonlinear disturbance observation method has achieved better control results.

5. Experiments

The accuracy of UVMS underwater operations can be judged by grasping control in hovering mode. We simulate sea cucumber fishing operations in a real marine environment to detect the depth, bow, and robot control accuracy of the designed control method for UVMS in a disturbed environment. In order to verify the functionality and reliability of UVMS, relevant tests have been carried out successively in swimming pools where artificial waves are created and real sea areas.

Simulating the sea cucumber fishing operation in the real sea area for pool test, which is different from the underwater industrial task. Most of the fishing operations are close to the seabed. What has a great impact on underwater fishing is the turbulent boundary layer between the whole flow layer (shallow water area) and the zero flow layer (seabed) produced by the ocean current. In order to simulate the disturbance effect of the turbulent layer, taking UVMS as the center, two 250 W aerated surge water cannons are set horizontally and vertically within 30 square meters of the

Figure 14: Ocean test.

critical point of water surface to achieve the effect of the water flow disturbance. The reference velocity is 5 m/s.

As shown in Figure 9, we carry out the fixed depth and fixed bow tests under the artificial disturbance environment of the pool are carried out, respectively. The nonlinear disturbance observation method is used to track the disturbance faced in the process of fixed depth and fixed bow movement in real time, and the adaptive sliding mode control method is used to adjust the power output to realize the tracking of the target path.

The desired depth in fixed depth mode is 1 m underwater. Figures 10 and 11 record the UVMS depth determination mode variables with or without nonlinear disturbance observation and control intervention for a period of time, save the data frame of the whole depth determination process, and obtain the motion curve of the whole depth determination process through postprocessing of the data. It is analyzed that under the disturbance environment, the variable error remains in the range of ±0.05 m after the intervention of the control algorithm, the average depth is 1.007 m, the system error is 0.007 m, and the control accuracy is excellent. It shows good depth determination performance. Due to the lack of effective judgment on the interval of disturbance, the system error of adaptive sliding mode depth determination control reaches 0.033 m.

Underwater operations are generally required to follow a certain direction. Due to the special underwater environment, the operator cannot directly judge the heading of the UVMS with the naked eye, so the heading needs to be obtained through the gyroscope and displayed in the ground monitoring software. However, UVMS is very susceptible to interference by ocean currents and often deviates from the actual set route. Therefore, it is necessary to estimate the disturbance force of the external environment to realize the real-time trajectory correction of UVMS.

Set the rated sailing speed to 1.5 m/s, refer to the depth-of-fix control on the previous vertical plane, and carry out a similar antidisturbance bow design for the UVMS fixed bow system, combining the conventional adaptive sliding mode method, and nondisturbance observer. The interventional adaptive sliding mode method is used for the comparative test of the fixed bow in the disturbed environment. As shown in Figures 12 and 13 in a disturbance environment, the conventional adaptive sliding mode method has a slightly poor direct navigation control accuracy and cannot track the desired trajectory in time, while the active disturbance

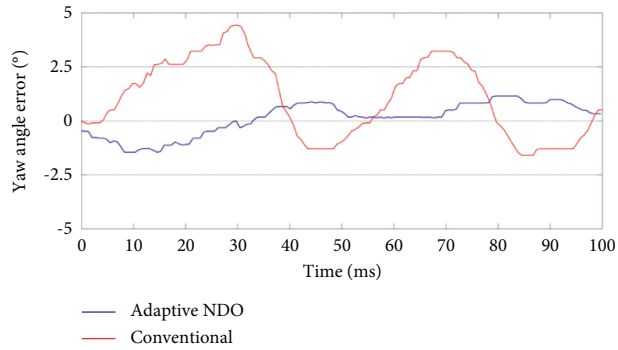

Figure 15: Comparison of heading error data.

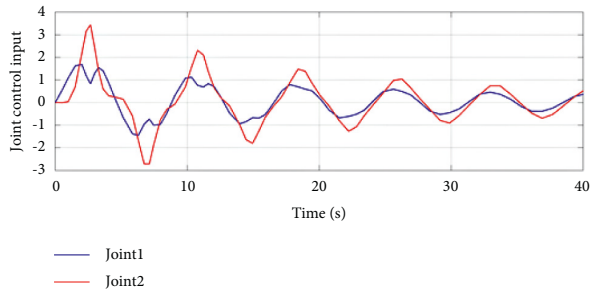

Figure 16: Robot input torque.

rejection algorithm can capture external disturbances in time and carry out active advance power intervention, which is helpful to improve UVMS fixed bow control performance.

Although the water tank experiment caused artificial disturbances, compared with the actual marine environment, the experimental environment and experimental data were relatively one-sided. As is shown in Figure 14, the team conducted a related underwater submarine test in an offshore area in Shandong.

The quantitative analysis of the heading determination mode of UVMS under different control methods can be obtained from Figure 15: compared with the ±5° yaw angle error under the conventional adaptive sliding mode control, the control method after NDO intervention has achieved a smoother yaw angle curve change, and the variation amplitude of yaw angle is controlled at ±2°, which timely suppresses the heading determination error caused by the disturbance of lateral environment during the movement of

UVMS, and achieves a better heading determination control effect.

The control of the manipulator in this subject is a visual servo control method. The vision system captures the target and performs relevant calibration, correction, stereo matching, ranging, and other steps to solve and obtain the rotation angle of each joint of the manipulator. The abovementioned relevant solution process is not the focus of this paper. We assume that the joint angles are known to judge the grasping accuracy in a disturbed environment.

As is shown in Figure 16, the input torque change diagram of each joint of the underwater manipulator is obtained in real time through the monitoring controller. As shown in Figure 16, the control input torque includes the approximation compensation for the coupling torque. When the disturbance comes, joint 1 generates a large compensation torque, and a large fluctuation occurs. Under the blessing of the control method, by increasing the input torque quickly. The joint angle and angular velocity are corrected to reflect the response performance of the control method. In the later control input, the control torque tends to a normal and stable amplitude, which highlights the excellent robustness of the designed back-stepping adaptive sliding mode method.

Experiments have verified that the control method can effectively compensate for sudden disturbances without significant pitch motion. It has strong robustness and provides a reliable and stable base for underwater manipulator operations.

6. Conclusions

Through research, by decoupling the UVMS dynamic model under disturbance, the vertical motion equation and trim motion equation related to depth determination control are obtained, and the adaptive sliding mode depth determination control involving nonlinear disturbance observation is studied. The ability of a nonlinear disturbance observer to approach external unknown disturbance is verified by simulation. The comparison diagram also shows that this method has a better disturbance compensation effect. It is verified that the nonlinear disturbance observation sliding mode adaptive control method has excellent control performance in UVMS fixed-depth control system.

Data Availability

The data used to support the findings of this study can be obtained from the corresponding author upon request.

Conflicts of Interest

The authors declare that there are no conflicts of interest regarding the publication of this paper.

Authors' Contributions

Chen Wei, associate professor, and master's supervisor has selected the "six talent peaks" in Jiangsu Province, the "mass entrepreneurship and innovation" talents in Jiangsu Province, and the training object of the scientific and technological innovation team of the "Blue Project" in Colleges and universities in Jiangsu Province. He is now a postdoctoral fellow of Southeast University, a member and senior member of the Youth Working Committee of the China Automation Society, and a member of the special committee of agricultural automation of Jiangsu Automation Society. He has been engaged in the research of robot control technology for a long time and presided over three national and provincial projects and five other projects. Won the third prize in the China machinery industry science and Technology Award and the third prize in Zhenjiang Science and Technology progress award. More than 30 relevant academic papers have been published, including more than 10 included in SCI/EI and 14 authorized invention patents.

Acknowledgments

This research was supported by the Modern Agriculture Project of Jiangsu province (BE2020406), the Changzhou Science and Technology Support Program (CE20212025), and the International Science and Technology Cooperation Project of Zhenjiang City (GJ2020009).

References

[1] P. Cieslak, P. Ridao, and M. Giergiel, "Autonomous underwater panel operation by GIRONA500 UVMS: a practical approach to autonomous underwater manipulation," in *Proceedings of the IEEE International conference on robotics and automation (ICRA)*, pp. 529–536, IEEE, Seattle, WA, USA, May 2015.

[2] W. Chen, T. Xu, J. Liu, M. Wang, and D. Zhao, "Picking robot visual servo control based on modified fuzzy neural network sliding mode algorithms," *Electronics*, vol. 8, no. 6, p. 605, 2019.

[3] Y. Dai and S. Yu, "Design of an indirect adaptive controller for the trajectory tracking of UVMS," *Ocean Engineering*, vol. 151, pp. 234–245, 2018.

[4] U. H. Shah, M. Karkoub, D. Kerimoglu, and H. Wang, "Dynamic analysis of the UVMS: effect of disturbances, coupling, and joint-flexibility on end-effector positioning," *Robotica*, vol. 39, no. 11, pp. 1952–1980, 2021.

[5] Z. Lin, H. D. Wang, M. Karkoub, U. H. Shah, and M. Li, "Prescribed performance based sliding mode path-following control of UVMS with flexible joints using extended state observer based sliding mode disturbance observer," *Ocean Engineering*, vol. 240, Article ID 109915, 2021.

[6] Y. Moon, J. Hong, S. Jin, J. Bae, and T. Seo, "Real-time UVMS torque distribution algorithm based on weighting matrix," *PLoS One*, vol. 16, no. 7, Article ID e0253771, 2021.

[7] X. Dong, C. Ren, S. He, L. Cheng, and S. Wang, "Finite-time sliding mode control for UVMS via TS fuzzy approach," *Discrete And Continuous Dynamical Systems-S*, 2021.

[8] J. Gao, X. Liang, Y. Chen, L. Zhang, and S. Jia, "Hierarchical image-based visual serving of underwater vehicle manipulator systems based on model predictive control and active disturbance rejection control," *Ocean Engineering*, vol. 229, Article ID 108814, 2021.

[9] S. Sagara and R. Ambar, "Performance comparison of control methods using a dual-arm underwater robot-Computed torque based control and resolved acceleration control for

UVMS," in *Proceedings of the IEEE/SICE International Symposium on System Integration (SII)*, pp. 1094–1099, IEEE, Honolulu, HI, USA, January 2020.

[10] E. Simetti, R. Campos, D. D. Vito et al., "Sea mining exploration with an UVMS: experimental validation of the control and perception framework," *IEEE*, vol. 26, no. 3, pp. 1635–1645, 2021.

[11] S. Heshmati-Alamdari, C. P. Bechlioulis, G. C. Karras, A. Nikou, D. V. Dimarogonas, and KJ. Kyriakopoulos, "A robust interaction control approach for underwater vehicle manipulator systems," *Annual Reviews in Control*, vol. 46, pp. 315–325, 2018.

[12] W. J. Marais, S. B. Williams, and O. Pizarro, "Go with the flow: energy minimising periodic trajectories for UVMS," in *Proceedings of the International Conference on Robotics and Automation (ICRA)*, vol. 3, p. 4, Philadelphia, PA, USA, May 2022.

[13] C. Yang, F. Yao, M. Zhang, Z. Zhang, Z. Wu, and P Dan, "Adaptive sliding mode PID control for underwater manipulator based on legendre polynomial function approximation and its experimental evaluation," *Applied Sciences*, vol. 10, no. 5, p. 1728, 2020.

[14] Q. Tang, Y. Hong, Z. Deng, D. Jin, and Y. Li, "Research on sliding mode control of underwater vehicle-manipulator system based on an exponential approach law," in *Proceedings of the International Conference on Swarm Intelligence*, pp. 607–615, Springer, Belgrade, Serbia, July 2020.

[15] M. Cai, Y. Wang, S. Wang, R. Wang, and M. Tan, "ROS-based depth control for hybrid-driven underwater vehicle-manipulator system," in *Proceedings of the Chinese Control Conference (CCC)*, pp. 4576–4580, IEEE, Guangzhou, China, July 2019.

[16] C. H. F. d Santos, M. U. Cildoz, M. H. Terra, and ER. De Pieri, "Backstepping sliding mode control with functional tuning based on an instantaneous power approach applied to an underwater vehicle," *International Journal of Systems Science*, vol. 49, no. 4, pp. 859–867, 2018.

[17] Y. Wei, Z. Zheng, Q. Li, Z. Jiang, and P. Yang, "Robust tracking control of an underwater vehicle and manipulator system based on double closed-loop integral sliding mode," *International Journal of Advanced Robotic Systems*, vol. 17, no. 4, Article ID 172988142094177, 2020.

[18] G. V. Lakhekar and L. M. Waghmare, "Robust maneuvering of autonomous underwater vehicle: an adaptive fuzzy PI sliding mode control," *Intelligent Service Robotics*, vol. 10, no. 3, pp. 195–212, 2017.

[19] E. Sebastián and M. A. Sotelo, "Adaptive fuzzy sliding mode controller for the kinematic variables of an underwater vehicle," *Journal of Intelligent and Robotic Systems*, vol. 49, no. 2, pp. 189–215, 2007.

[20] Y. Wang, B. Chen, and H. Wu, "Joint space tracking control of underwater vehicle-manipulator systems using continuous nonsingular fast terminal sliding mode," *Proceedings of the Institution of Mechanical Engineers - Part M: Journal of Engineering for the Maritime Environment*, vol. 232, no. 4, pp. 448–458, 2018.

[21] S. Mobayen, O. Mofid, S. U. Din, and A Bartoszewicz, "Finite-time tracking controller design of perturbed robotic manipulator based on adaptive second-order sliding mode control method," *IEEE Access*, vol. 9, Article ID 71159, 2021.

[22] O. Mofid, S. Mobayen, and A. Fekih, "Adaptive integral-type terminal sliding mode control for unmanned aerial vehicle under model uncertainties and external disturbances," *IEEE Access*, vol. 9, Article ID 53255, 2021.

[23] S. Miao, B. Zhang, M. Wang, X. Wang, and Y. Shen, "Adaptive exponential time-varying sliding mode control of airborne photoelectric stabilization platform based on disturbance observer," *Journal of Ordnance Engineering*, pp. 1–12, 2022.

[24] X. Bai, Y. Wang, S. Wang, R. Wang, and W. Wang, "Modeling and analysis of an underwater biomimetic vehicle-manipulator system," *Science China Information Sciences*, vol. 65, 2022.

[25] G. Levitin, L. Xing, and Y. Dai, "Co-residence based data theft game in cloud system with virtual machine replication and cancellation," *Reliability Engineering & System Safety*, vol. 222, Article ID 108415, 2022.

[26] S. M. Youssef, M. A. Soliman, M. A. Saleh, M. A. Mousa, M. Elsamanty, and AG. Radwan, "Underwater soft robotics: a review of bioinspiration in design, actuation, modeling, and control," *Micromachines*, vol. 13, no. 1, p. 110, 2022.

[27] S. Mobayen and F. Tchier, "An LMI approach to adaptive robust tracker design for uncertain nonlinear systems with time-delays and input nonlinearities," *Nonlinear Dynamics*, vol. 85, no. 3, pp. 1965–1978, 2016.

[28] X. Zhang, X. Liu, Y. Wang, C. Liu, N. Zhang, and J. Lu, "Exploration of cortical inhibition and habituation in insomnia: based on CNV and EEG," vol. 204, Methods, 2022.

[29] W. Chen, X. Li, H. Ge, L. Wang, and Y. Zhang, "Trajectory planning for spray painting robot based on point cloud slicing technique," *Electronics*, vol. 9, no. 6, p. 908, 2020.

[30] W. Chen, J. Zhang, B. Guo, Q. Wei, and Z. Zhu, "An apple detection method based on des-YOLO v4 algorithm for harvesting robots in complex environment," *Mathematical Problems in Engineering*, vol. 2021, no. 10, 12 pages, Article ID 7351470, 2021.

[31] F. Plasencia-Balabarca, E. Mitacc-Meza, M. Raffo-Jara, and S. C. Carlos, "A flexible UVM-based verification framework reusable with avalon, AHB, AXI and wishbone bus interfaces for an AES encryption module," in *Proceedings of the IEEE Latin American Test Symposium (LATS)*, pp. 1–4, IEEE, Santiago, Chile, March 2019.